Describing the dynamic response of a ceramic: The search for universality in fragmentation statistics

S. Levy[1], J.F. Molinari[1]
[1]LSMS, IS, ENAC, *Ecole Polytechnique Federale de Lausanne, Lausanne, Switzerland*

1. Introduction

Submitted to dynamic loadings, ceramics break into many fragments. Even with the considerable progress of the last decades, fragmentation remains misunderstood. Indeed, the effect of the ceramic microstructure on dynamic fragmentation is a current research issue. In quasi-statics, the general agreement is that the weakest link theory applies and predicts that fracture occurs at the weakest flaws: the structure breaks into few fragments. On the contrary, understanding the role of the defects on dynamic fragmentation is still an open issue [10]. Ceramics are usually brittle and exhibit a large population of defects. In dynamics, not only the weakest flaws but a critical population of flaws initiates. It generates local damage and potentially failure at several fracture sites: the structure breaks into many fragments.

Besides the complications brought by the microstructure, fragmentation remains a complex physical phenomenon that is usually described either using statistics or physicals. Physically-based theories have first emerged during World War II when Mott studied shell fragmentation [8]. He described the process dynamically: when a fracture occurs at some point, it releases a compression wave which protects the encompassed part of the body. Later, this idea of obscuration waves has been reused theoretically by Hild et al. in [2], Drugan in [3] and numerically by Zhou et al. in [12]. [3] and [12] have both have enriched the concept by discretizing space at the potentially fracture sites. Cohesive elements model crack opening, which is not instantaneous anymore. Drugan's theoretical approach leads to the definition of a characteristic fragment size, redefined here in section 4. Yet, analytical derivations remain limited to model the complex wave interaction network that takes place during the process. The main advantage of numerical simulations is their ability to handle precisely these non-linearities. Zhou et al. ran simulations based on the method of characteristics and ended up with promising results on fragment size distributions. Though, they did not include the microstructure of the material and did not focus on its effect on dynamic fragmentation.

Similarly, energy-based models are part of the physically-based class and do not attempt to fill in this gap. These theories use energy criteria to relate material properties and loading rates to the characteristic fragment size. The most well-known is Grady's [6], who assumed that the local kinetic energy is fully converted into fracture energy. Glenn and Chudnovsky [5] generalized this

formulation to quasi-static regime where the strain energy released by the weakest link failure dominates. Due to their simplicity, these formulations have been conveniently used in most engineering applications related to dynamic fragmentation.

Finally, the second class of approaches is based on statistics, which are obviously an appropriate tool for predicting fragment size and velocity distributions. The mathematical derivation is however not direct. Over the past decades, theoretical, numerical, and experimental theories have emerged. Although they all predict an exponential law for the cumulative density function of the fragment sizes, their characteristic parameters differ.

In this paper, we aim at describing the effect of the population of defects on dynamic fragmentation. Motivated by its simplicity, we have focused our work on the one-dimensional expanding ring experiment. The finite-element method coupled to cohesive interfaces model the evolution of the process. Given their density and their initial distribution, defects are randomly distributed along the structure. After the numerical definition of the problem, the physics of the phenomenon are described by analyzing the energy terms. The effect of the population of defects is then underlined by studying the average fragment size and the distribution of fragment sizes.

2. Numerical methodology

21. The expanding ring test

First defined by Mott in the forties [9], the expanding ring experiment is an easily conductible test. Numerous experimental results are consequently available for ductile and brittle materials. Moreover, since the ring is a periodic structure with negligible thickness, neither boundary effects nor crack propagation determine the process evolution. The physical interpretation is thus focused on the initiation of the cracks, crucial in dynamics and inherently related to the population of defects. In practice, the mesh has one element in the thickness so that the numerical calculations do not allow crack propagation.

The test consists in studying the fragmentation of a heterogeneous brittle ring whose motion is imparted by some radial impulse, as illustrated in figure (1). Just before the first crack initiates at the weakest link, the ring is subjected to a uniform strain rate $\dot{\varepsilon} = \frac{radial\ velocity}{radius}$. Then, release waves propagate away from the damaged site, relieving the tension in its neighbourhood and avoiding encompassed sites to initiate. Fragmentation is complete when the release waves have unloaded the entire ring. In this study, we simulate the fragmentation of a ceramic of length $2\,cm$ with volumetric mass $\rho = 2750 kg.m^{-3}$, approximate failure strength $\sigma_c = 300 MPa$ and approximate fracture

toughness $G_c = 100 N.m^{-1}$. Everywhere but at the fracture sites, the material behaves elastically with Young's modulus $E = 271 GPa$ so that the elastic wave speed is $c = 10000\, m.s^{-1}$. The expansion of the ring is simulated with the finite-element method. Cohesive elements handle crack initiation, opening, closing and failure.

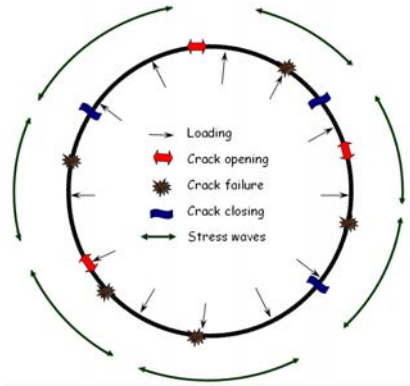

Figure 1 : The expanding ring test

2.2. The cohesive methodology

Initially the ring is crack free. As the stress increases, cohesive elements are dynamically inserted into the mesh, at any time, any point, where the local stress exceeds the local critical value called cohesive strength:

$$\sigma(X) \geq \sigma_c(X) \Rightarrow \quad \textit{Insertion of a cohesive element}$$

The insertion framework follows the one described by Camacho and Ortiz in [1]. Once initiated, the crack either grows or closes, governed by the linear cohesive behaviour defined in figure (2). Cracks communicate through elastic waves that propagate in both directions.

The crack opening governs the evolution of the crack. It is decomposed into normal δ_n and shearing δ_s slidings:

$$\delta_{coh} = \sqrt{\delta_n^2 + \beta \delta_s^2}$$

In our case, as the problem is essentially one dimensional, $\delta_{coh} = \delta_n \quad (\beta = 0)$.

The cohesive behaviour is guided by:

$$\begin{cases} \dfrac{\sigma_{coh}}{\sigma_c} = 1 - \dfrac{\delta_{coh}}{\delta_c}, \ \textit{for } \dot{\delta}_{coh} > 0, \ \delta_{coh} = \delta_{\max}, D < 1.0 \\ \dfrac{\sigma_{coh}}{\sigma_c} = 1 - \dfrac{\delta_{\max}}{\delta_c}, \ \textit{for } \delta_{coh} < \delta_{\max}, D < 1.0 \end{cases}$$

σ_c is the cohesive strength of the cohesive element, δ_c is its critical opening distance. The maximum attained opening is $\delta_{\max}$, the effective opening is δ_{coh}. The first equation applies when the crack opens while the second controls the closing and reopening.

The parameter $\delta_{\max}$ is used as an internal variable to define the local damage:

$$D = \max\left(\delta_{\max} / \delta_c \, , 1.0 \right)$$

When D is equal to 1, the cohesive element is totally broken and has released the local toughness $G_c = \frac{\sigma_c \delta_c}{2}$. When it is partially damaged, it has dissipated $E_{dis} = D^2 G_c$ and stores $R_{rec} = \sigma_{coh} \delta_{coh}$ (where *rec* stands for recoverable).

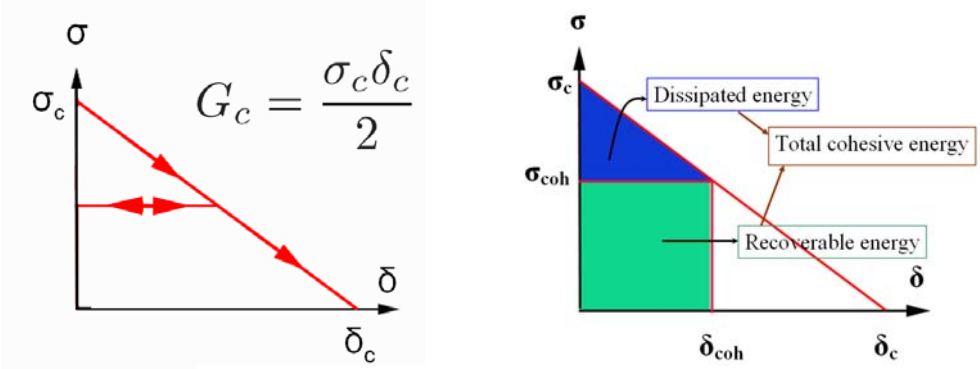

Figure 2 : The adopted cohesive law and its related energies

This numerical scheme is defined locally; each fracture site is defined by two parameters σ_c and G_c. Thus, it makes physical sense to use these parameters for the definition of the defect population.

2.3. Population of defects

Each fracture site is associated to a given value of cohesive strength σ_c. We make the hypothesis that the population of defects determines the distribution of σ_c. Two parameters have to be defined: the density of defects and the distribution of the values of σ_c. The density of defects is the number of randomly spaced fracture sites (pores or inclusions or microcracks …) per unit length. At a given applied stress, some of these defects are weak enough to initiate. This condition is determined by the value of $\sigma_c(\underline{X})$ statistically defined by the probability density function.

In this study, three types of probability density functions are studied: uniform, normal and Weibull [11] distributions. They are entirely defined by their mean (symbol *m* in fig(3)) and their standard deviation (symbol *s*). Large and small standard deviations are compared in order to link nearly homogeneous and highly heterogeneous materials.

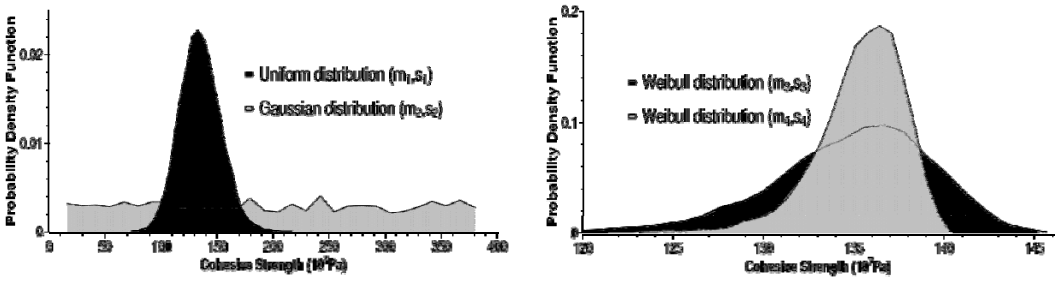

Figure 3 : Probability density functions of some defect populations
$m_1=m_2=344MPa$, $s_1=140MPa$, $s_2=21MPa$, $m_3=347MPa$, $s_3= 5.7MPa$, $m_4=3.86MPa$, $s_4=3MPa$

The following section focuses on energy terms in order to apprehend the physics of the phenomenon. Then, we highlight the influence of the population of defects and the loading rate on the average fragment size. Finally, our main results on fragment size distributions are presented.

3. Energy terms

When fragmentation processes, kinetic and elastic energies are partially converted into cohesive energy. Figure (4) illustrates the evolution of the energy for a loading rate equal to $1000\,m.s^{-1}$. The potential energy increases until the peak stress after which most fragments are generated. Then, it oscillates around a non-zero value, in the opposite way as the kinetic energy. Each fragment has a residual kinetic energy (fragments are flying away and stress waves still propagate) and a residual potential energy (fragments are ringing because of their elastic bulk properties). The dissipated cohesive energy is an increasing function of time that stabilizes when no more fragments is generated.

These energy terms depend both on the strain rate and the population of defects. The weakest defect obviously drives the maximum potential energy; the behaviour after this peak depends on the fracture process. Figure (5) gives the example of the time evolution of the potential energy of two uniform distributions loaded at $10^5 ms^{-1}$.

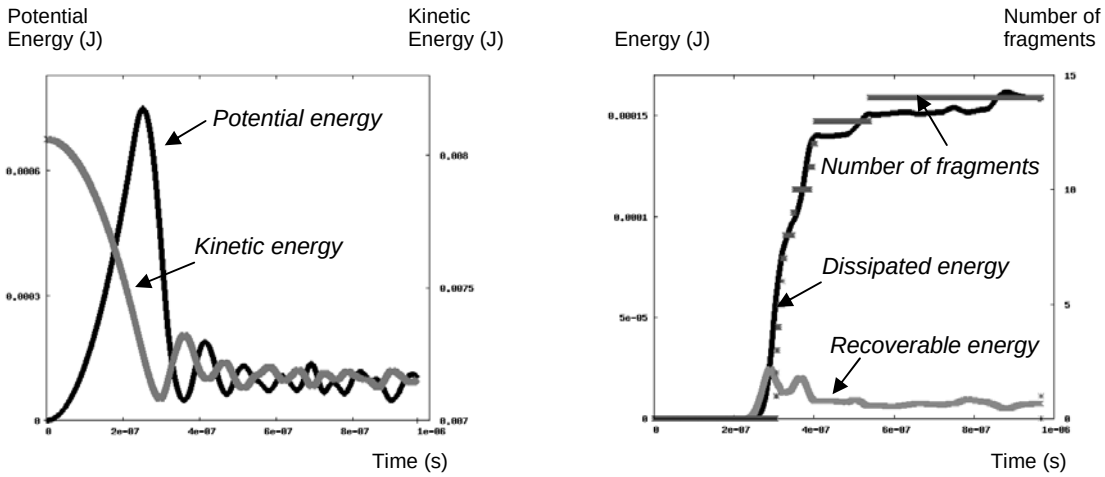

Figure 4 : Time evolution of the energy terms and number of generated fragments when the loading rate is 1000m/s

Although they have the same mean, one has a low standard deviation (the ring is nearly homogeneous, grey plot in fig(5)); the other one has a large standard deviation (the ring is highly heterogeneous, dark plot in fig(5)). In the homogeneous case, the potential energy reaches the peak stress and decreases slowly afterwards. The process characteristic time is larger than in the heterogeneous case. Energy terms represent well the fragmentation process. Yet, they do not describe it quantitatively; the following sections detail fragment characteristics.

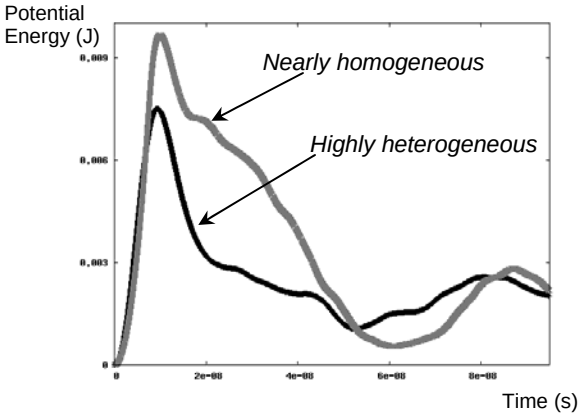

Figure 5 : Potential energy evolution for two uniform defect population with same mean and different standard deviation

4. Influence of the defects and the strain rate on the average fragment size

Following the idea of Zhou et al. in [14], we consider that the average fragment size characterizes the ring fragmentation. Several distributions of defects have been tested: the density of defects, the shape of the distribution, its standard deviation and its mean influence fragmentation. For instance, figure (6) represents the effect of the density on the average fragment size for different strain rates. The distribution is uniform with mean 344MPa and standard deviation 140MPa. Zhou et al. proposed a normalization of the axis, depending on the material properties. The x-axis and y-axis are respectively divided by $\dot{\varepsilon}_0$ and by s_0

$$\text{where } s_0 = \frac{G_c E}{\sigma_c^2} \text{ and } \dot{\varepsilon}_0 = \frac{c.\sigma_c}{E.s_0}$$

When the ring is not homogeneous, this normalization does not gather anymore the plots in a single universal law. A new normalization is to be defined by including the microstructure properties.

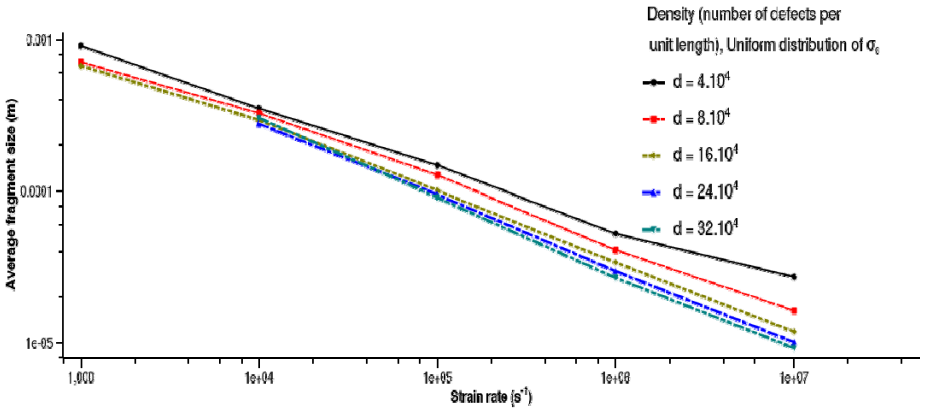

Figure 6 : Average fragment size versus strain rate for different density, for a given distribution (uniform with mean 344MPa and standard deviation 140 MPa)

5. Influence of defects and strain rate on the distribution of fragments

Once the average fragment size is computed, one can relevantly consider the distribution of fragment sizes. In the following results, the x-axis has been normalized by the average fragment size. Following most previous works on fragmentation, we then fit the curves with the cumulative density function of size s defined by:

$$\frac{N(s)}{N_{fragment}} = \exp\left(-\left(\frac{s}{\alpha\, s_{average}}\right)^m\right)$$

Grady [7] used Poisson statistics and derived the exponent value 1. Mott [9] gathered experimental data and showed that the exponent is ½. Other experiments [4] exhibit an exponent larger than 2. Numerical results from Zhou et al. [12, 13] predicted the exponent 2. In our case, we observe a slightly different exponent. Indeed, at first glance, the exponent m does not vary considerably and ranges the values 2.5 +/- 0.3. Yet, these results are to be complemented in order to confirm this trend. If it is confirmed, it would mean that the only determining parameter is the average fragment size.

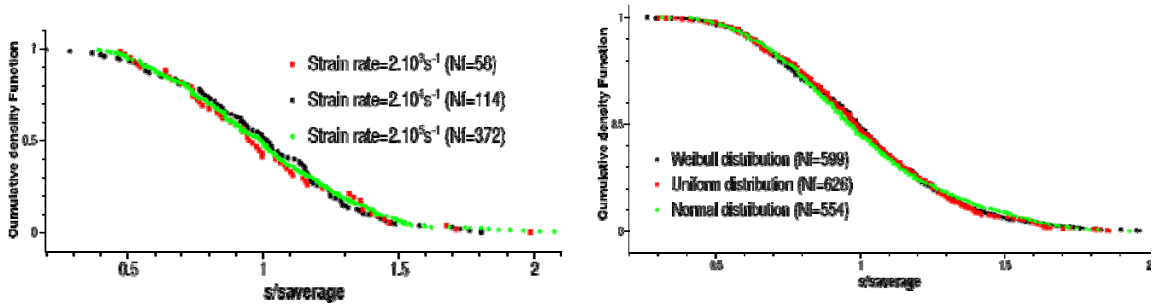

Figure 6: Cumulative density function of the fragment sizes. Nf is the number of fragments On the left, same normal distribution, density and strain rate vary. On the right, same strain rate, density and distribution type vary.

6. Summary and discussion

In this paper, we have developed a methodology to analyze fragmentation of a heterogeneous ring. The choice of this quasi one-dimensional structure was made for simplicity in order to focus on heterogeneity effects. The finite-element scheme modelled the elastic temporal evolution of the bulk while cohesive linear elements managed crack initiation, opening, closure and failure. This numerical framework provided an effective mean of simulating stress wave interactions and their effect on fragmentation. The population of defects was defined both by the density of flaws and by the distribution of their critical stresses.

Energy terms helped the visualization of these stress waves and the evolution of the energy dissipated by the numerous fractures. Then, we related each numerical test to the average fragment size, in order to quantify the effect of the loading rate and the defects on fragmentation. Both had an obvious effect that increased with the loading rate. Since the normalization proposed by Zhou et al. only considered homogeneous materials, it did not apply to our problem. A new normalization must be defined and include some relevant parameters of the population of defects. Finally, we looked at the distribution of fragment sizes and observed that after normalizing the x-axis, they follow a universal exponential law which exponent is around 2.5. This result is promising and still needs to be confirmed by other developments. Monte-Carlo simulations are to be run to give a statistical better understanding of the relation between the fragmentation process and the material microstructure.

Acknowledgments

The authors gratefully acknowledge the support from ARO through the grant number W911NF-08-1-0150, and ARL through University of Nebraska Lincoln (grant number W911NF-04-2-0011).

References

[1] G.T. Camacho, M. Ortiz, Computational modeling of impact damage in brittle materials, International Journal of solids and structures (33) (1996), 2899-2938
[2] C. Denoual, G. Barbier, F. Hild, A probabilistic approach for fragmentation of brittle materials under dynamic loading, Mechanics of solids and structures (325) (1997)
[3] W.J. Drugan, Dynamic fragmentation of brittle materials: analytical mechanics-based models, Journal of the mechanics and physics of solids (49) (2001), 1181-1208
[4] J.J. Gilvarry, B.H. Bergstrom, Fracture of brittle solids .2. Distribution function for fragment size in single fracture (Experimental), Journal of applied physics (32) (1961), 400
[5] L.A. Glenn, A. Chudnovsky, Strain-energy effects on dynamic fragmentation; Journal of applied physics (59) (1986), 1379-1380
[6] D.E. Grady, Local inertial effects in dynamic fragmentation, Journal of applied physics (53) (1982)
[7] D.E. Grady, Particle-size statistics in dynamic fragmentation, Journal of applied physics (68) (1990), 6099-6105
[8] N.F. Mott, Fragmentation of shell cases, Proceedings of the royal society of London series A-mathematical and physical sciences (189) (1947), 300-308
[9] N.F. Mott, Fragmentation of H.E. Shells: A Theoretical Formula for the distribution of Weights of Fragments, United Kingdom Ministry of Supply (1943)
[10] B. Paliwal, K.T. Ramesh, An interacting micro-crack damage model for failure of brittle materials under compression, Journal of the Mechanics and Physics of Solids(56) (2008), 896-923.
[11] W. Weibull, A statistical Theory of Strength of Materials, Proceedings of the Ingeniors Vetenskapsakad (1939),151
[12] F. Zhou, J.F. Molinari, K.T. Ramesh, Analysis of the brittle fragmentation of an expanding ring, Computational Materials Science(37) (2006),74-85
[13] F. Zhou, J.F. Molinari, K.T. Ramesh, Effects of material properties on the fragmentation of brittle materials, International Journal of Fracture (139) (2006), 169-19.
[14] F. Zhou, J.F. Molinari, K.T. Ramesh, Characteristic fragment size distributions in dynamic fragmentation, Applied Physics letters (88) (2006)